Full-Span Tiltrotor Aeroacoustic Model (FS TRAM) Overview and Initial Testing

Megan S. McCluer
NASA Ames Research Center
Moffett Field, CA

Jeffrey L. Johnson
Aerospace Computing, Inc.
Mountain View, CA

ABSTRACT

The Full-Span Tiltrotor Aeroacoustic Model (FS TRAM) is a dual-rotor, powered wind tunnel model with extensive instrumentation for measurement of structural and aerodynamic loads. The model has been developed to investigate tiltrotor aeromechanics and to generate a comprehensive database for validating analyses, as well as a research platform for studying current and future tiltrotor designs. This paper describes the Full-Span TRAM test stand and the first set of data obtained at the NASA Ames Research Center 40- by 80-Foot Wind Tunnel test conducted in late 2000. Limited results are presented and recommendations for future testing are provided. This model has been established as a valuable national asset for tiltrotor research.

INTRODUCTION

The tiltrotor is a versatile aircraft which can fly with the speed and range of a turboprop airplane while also having the vertical take-off and landing capability of a helicopter. Wind tunnel testing of tiltrotor models increases the understanding of tiltrotor aerodynamics, dynamics, performance, and acoustics, and enables the development of advanced computational design tools. Wind tunnel data can also be used to improve simulation models and investigate detailed conditions that are too arduous to obtain in flight test. The Full-Span Tilt Rotor Aeroacoustic Model (FS TRAM), shown in Figure 1, is a 1/4-scale representation of the V-22 Osprey aircraft (Figure 2) and was tested at the NASA Ames Research Center 40- by 80-Foot Wind Tunnel in late 2000. The first full-span test served primarily as a complete system build-up and checkout. Model, motor, and rotor system controls and measurements were built, installed, and verified. Limited test data were obtained on rotor performance, blade structural loads, and wing static pressures. Some laser light sheet flow visualization images and acoustics data were also obtained. Additional testing will provide the full-span tiltrotor data the rotorcraft community requires, since isolated and semi-span model testing do not fully address all tiltrotor aeromechanics issues. The long-term goal of the FS TRAM is to be a tiltrotor research tool for future testing by the U.S. industry and Government.

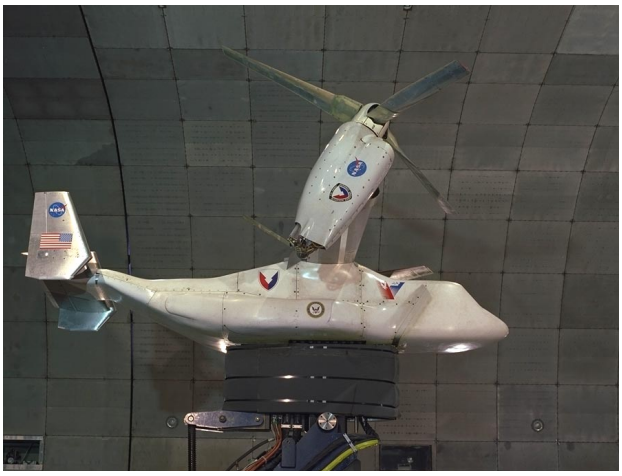

Figure 1. The Full-Span TRAM mounted in the NASA Ames 40- by 80-Foot Wind Tunnel.

Figure 2. The V-22 Osprey tiltrotor aircraft during shipboard operational evaluations. (U.S. Navy Photo)

Presented at the American Helicopter Society Aerodynamics, Acoustics, and Test and Evaluation Technical Specialists' Meeting, San Francisco, CA, January 23-25, 2002.

Report Documentation Page

Form Approved
OMB No. 0704-0188

1. REPORT DATE	2. REPORT TYPE	3. DATES COVERED
2002		**00-00-2002 to 00-00-2002**

4. TITLE AND SUBTITLE	5a. CONTRACT NUMBER
Full-Span Tiltrotor Aeroacoustic Model (FS TRAM) Overview and Initial Testing	5b. GRANT NUMBER
	5c. PROGRAM ELEMENT NUMBER
6. AUTHOR(S)	5d. PROJECT NUMBER
	5e. TASK NUMBER
	5f. WORK UNIT NUMBER
7. PERFORMING ORGANIZATION NAME(S) AND ADDRESS(ES) **Army/NASA Rotorcraft Division,Army Aviation and Missile Command,Aeroflightdynamics Directorate (AMRDEC), Ames Research Center,Moffett Field,CA,94035**	8. PERFORMING ORGANIZATION REPORT NUMBER
9. SPONSORING/MONITORING AGENCY NAME(S) AND ADDRESS(ES)	10. SPONSOR/MONITOR'S ACRONYM(S)
	11. SPONSOR/MONITOR'S REPORT NUMBER(S)

12. DISTRIBUTION/AVAILABILITY STATEMENT
Approved for public release; distribution unlimited

13. SUPPLEMENTARY NOTES
Presented at the American Helicopter Society Aerodynamics, Acoustics, and Test and Evaluation Technical Specialists' Meeting, San Francisco, CA, January 23-25, 2002

14. ABSTRACT
The Full-Span Tiltrotor Aeroacoustic Model (FS TRAM) is a dual-rotor, powered wind tunnel model with extensive instrumentation for measurement of structural and aerodynamic loads. The model has been developed to investigate tiltrotor aeromechanics and to generate a comprehensive database for validating analyses, as well as a research platform for studying current and future tiltrotor designs. This paper describes the Full-Span TRAM test stand and the first set of data obtained at the NASA Ames Research Center 40- by 80-Foot Wind Tunnel test conducted in late 2000. Limited results are presented and recommendations for future testing are provided. This model has been established as a valuable national asset for tiltrotor research.

15. SUBJECT TERMS

16. SECURITY CLASSIFICATION OF:			17. LIMITATION OF ABSTRACT	18. NUMBER OF PAGES	19a. NAME OF RESPONSIBLE PERSON
a. REPORT **unclassified**	b. ABSTRACT **unclassified**	c. THIS PAGE **unclassified**	**Same as Report (SAR)**	**17**	

Prior to the complete full-span model construction, the right rotor and nacelle were tested in the Duits-Nederlandse Windtunnel (DNW) in 1998. The purpose of the rotor test was to acquire isolated rotor performance, blade pressure and acoustic data. Figure 3 shows the isolated rotor in the DNW. References 1 - 8 discuss the TRAM/DNW test and the results.

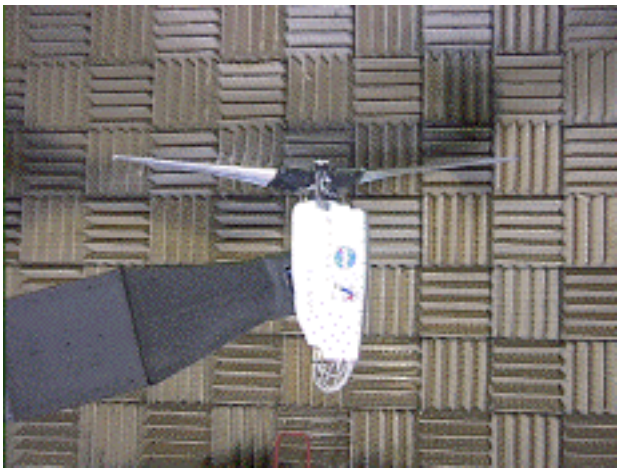

Figure 3. Isolated TRAM rotor in DNW.

The primary objective for the FS TRAM 40- by 80-Foot Wind Tunnel entry was to complete the full-span build-up and development of the tiltrotor platform. Prior to obtaining research data, the electrical, mechanical, controls, instrumentation, data acquisition, and software systems were integrated, calibrated, and verified. The model was installed in the test section on a vertical strut and pitch mechanism. Figures 1 and 4 show the FS TRAM mounted in the test section. Figure 4 shows the scale of the test section with respect to the model.

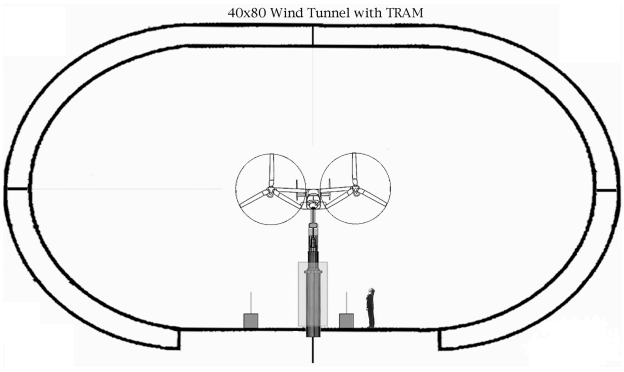

Figure 4. FS TRAM shown to scale in the 40- by 80-foot test section.

It was not a trivial effort to insure proper operation of, and communication between, the data channels, the aircraft control systems, the facility control systems, the data acquisition system, the safety of flight monitoring system, the acoustic traverse controller, the wing pressure system, the laser equipment, strobes, cameras, and the wind tunnel data system. This was accomplished, and limited research data were obtained before the test ended prematurely due to an oil pump component failure.

Rotor and vehicle performance measurements were taken in addition to wing pressures, acoustics, and flow visualization. Hover, helicopter-mode forward flight, and airframe aerodynamic runs were performed. Performance data were acquired for three different tunnel speeds and four different rotor tip path plane angles. Figure 5 shows the matrix of test conditions where data were acquired for different tip-path-plane angles of attack, Atpp.

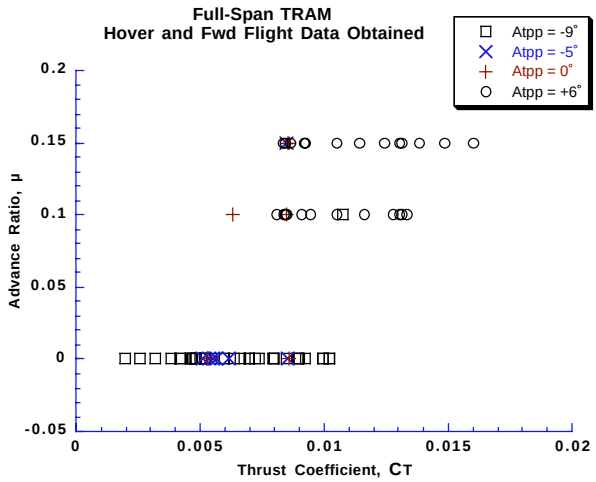

Figure 5. Full-Span TRAM matrix of test conditions where data were acquired during initial 40- by 80-Foot Wind Tunnel testing.

This paper will describe the 40- by 80-Foot Wind Tunnel, the FS TRAM model including systems and components, test measurements, data reduction, data quality issues, and results.

Description of the 40- by 80-Foot Wind Tunnel

The 40- by 80-Foot Wind Tunnel is a closed circuit, single-return, closed test section facility with a 300 knot wind speed capability. The test section measures 40 feet high by 80 feet wide and 80 feet long and has semicircular side walls, as seen in Figure 4. The wind tunnel facility has undergone several major modifications to improve performance, raise test section speed, and improve acoustic treatment, since initial operation began in 1944. The 80- by 120-Foot Wind Tunnel test section leg was added in the mid-1980's along with upgraded fan-drive motors. The tunnel is currently driven by six 40-foot diameter fans, each powered by a 22,500 HP motor. Reference 9 summarizes the performance and test section flow characteristics. A new acoustic liner for the 40- by 80- Foot Wind Tunnel test section, completed in early 1999, is designed to have a minimum of 90% acoustic energy absorption from 80 Hz to 20 kHz. References 10

and 11 present the design, implementation and resulting acoustic characteristics and flow quality of the new test section. Reference 12 describes the facility and various types of rotor testing capability. The 40- by 80-Foot and 80- by 120-Foot Wind Tunnels are well suited for large and full-scale rotor testing due to their size, speed range and attenuation of low frequency noise.

A traversing microphone system was available for making acoustic surveys of the flowfield during testing. The Acoustic Survey Apparatus (ASA) consists of a system of rails mounted to the test section floor on which microphones or microphone rakes can be mounted. The system design provides for a wide variety of survey options including streamwise and cross-stream traverse capability. For the FS TRAM test, two streamwise ASA rails were installed each supporting a wing-shaped rake carrying six microphones. Figure 6 shows the FS TRAM installed in the test section, the two ASA traverse tracks with microphone wings can be seen in the foreground.

Figure 6. The FS TRAM installed in the 40- by 80-Foot Wind Tunnel showing the acoustic traverse rails and microphone wings.

FS TRAM MODEL DESCRIPTION

The FS TRAM is a complex integration of structure, utilities, controls, instrumentation, and monitoring systems. This section describes the structural model and mount, the aerodynamic control surfaces and consoles, the drivetrain, utilities, hub assembly, rotor blades, and balances. Considerable information in this section was obtained from (and more detail can be found in) References 2, 3 and 13.

Basic Structure

The FS TRAM structure is comprised of a primary steel and aluminum chassis enclosed by non-structural fiberglass skins nominally conforming to the outer mode line of a 1/4-scale V-22 Osprey tiltrotor aircraft. The primary strongback consists of a wing center spar, pedestal and empennage tail boom. The center spar saddles the pedestal and supports the cantilevered loads of the wing and rotors. The pedestal also provides the structural base for the empennage tail boom structure, which transfers loads from the horizontal and vertical stabilizers. The wing spar transmits all of the loads from the rotor, nacelle and wing into the fuselage. The wing spar and tilt axis are not swept; wing sweep is accomplished via tapered leading and trailing edge components bolted to the straight spar. The hollow leading edge assembly forms a channel for routing instrumentation and control wiring. The wings are structurally rigid, designed to maximize the dynamic stability margin of the model. The wing and all other model structural components are designed to maintain a factor-of-safety greater than four during all phases of testing up to 300 knots. The rotor nacelles have a tilt range of 0 deg (airplane mode) to 95 deg in 5-deg increments and are manually adjusted. Figure 7 identifies the major components of the full-span model.

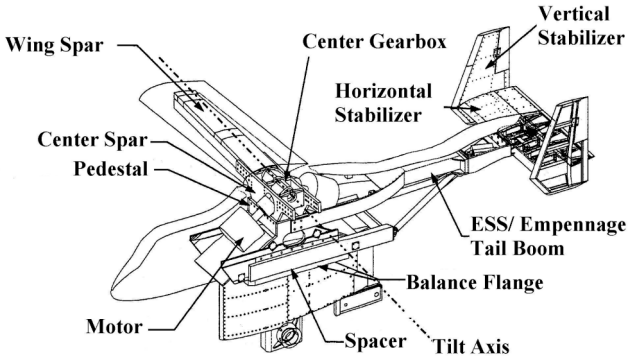

Figure 7. Full-span TRAM components

Mount

A bayonet strut connects the non-metric side of the fuselage balance to the facility sting pitch mechanism, which permits model pitch rotation about a point 37.25" below the balance center. The pitch range for this test entry was -9 deg (nose down) to +18 deg (nose up). Figure 8 shows the pitch mechanism that changes the fuselage angle of attack. The rotor disc elevation, when in helicopter mode, was 21.8 feet above the floor. In airplane mode, the rotor hubs were 19.7 feet above the floor.

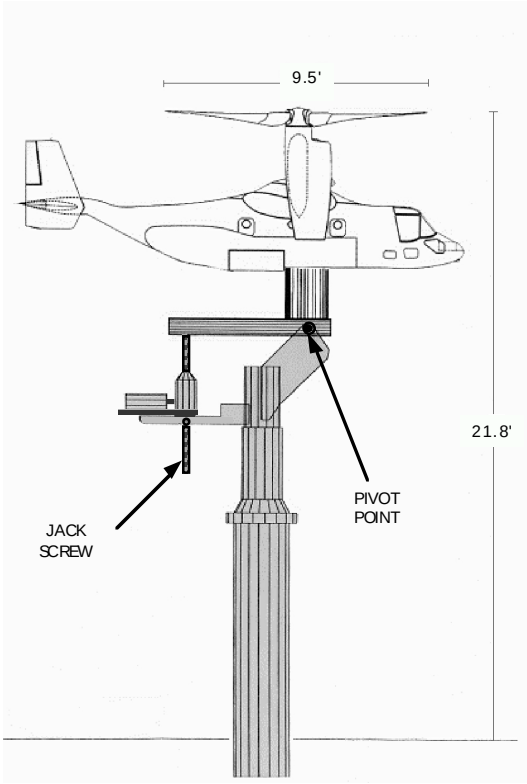

Figure 8. FS TRAM installed on the 40- by 80- Foot Wind Tunnel strut and pitch mechanism. (Aerodynamic fairing not shown.)

Control Surfaces

TRAM has movable inboard and outboard wing flaperons, which are driven by electro-mechanical actuators. Individual flap seals were fabricated to seal the gap between the wing and flaperons. The flaperons operate in one of two separate ranges, from –35 deg (flap trailing edge up) to +35 deg (trailing edge down) and from +35 deg to +100 deg. A linkage change on each flaperon is required to switch ranges. The model has a movable elevator with a range of –10 (trailing edge up) to +30 deg, (trailing edge down). The vertical stabilizers have ground-adjustable rudders. Rudder deflections are made with fixed-angle brackets for each deflection angle. The rudders were set at zero deflection throughout this test. The Fixed-Wing Control Console (FWCC) provides control of the flaperons and elevator from the wind tunnel control room. The flaperons can be driven independently or together.

Drive train

Two permanent-magnet, solid-state controlled, electric motors are located in the fuselage body, one forward and one aft of the wing. The motors are rated at 300 HP at 18,000 RPM and were built by Kaman Electromagnetics Corporation. Each motor is connected to a 90-degree center gearbox. The gearboxes are interconnected, mechanically linking the two rotors, similar to the cross-shaft in the wing of the full-scale aircraft. Power is transmitted from the center gearboxes out to the nacelle transmission via supercritical drive shafts located inside each wing spar. The drive train operates at high rotational speed to transfer power at safe torque levels through the shaft, since the shaft diameter is limited by the restricted space inside the wing spars. The nacelle transmission has a three-stage gear reduction (11.34:1) and turns 90 deg to drive the rotors at the proper RPM. The nacelle transmission reduces the drive train rotational speed to 1588 RPM, which corresponds to a rotor tip-speed of 790 ft/s, (the original design tip speed of the V-22). The nacelle transmission case also provides the structural load path to carry rotor forces and moments in the wing spar.

Utilities

A utility pump system, housed in the nose section of the fuselage, provides lubrication and cooling oil to the center gearboxes, the electric drive motors, and the sliprings. Oil is continuously filtered, cooled by heat exchangers, and re-circulated through the gearboxes. The nacelle transmissions have a similar mechanical driven system. A Utility Control Console (UCC) provides remote control of model utilities including the lubrication systems, the oil mist for motor bearings, cooling air for the rotating amplifier system, and the slipring cooling system fluid.

Rotor Control System

The custom Rotor Control Console (RCC) occupies two instrumentation bays and has fully redundant hardware and software. Kinematic equations representing TRAM control system geometry are programmed into the mixer software to convert operator joystick control inputs to appropriate actuator movement at the swashplate. The system has fault detection and fail-safe features, and rotor cyclic and collective displays. The console can be configured to control the isolated rotor or dual-rotor TRAM configuration. In dual-rotor mode, both rotors can be slaved together or controlled separately.

Rotating Amplifier System (RAS)

All rotating data channels on the right-hand side are input to a rotating amplifier system (RAS) (Ref. 14). The RAS is designed to provide signal conditioning and amplification of 256 channels and to provide up to 128 unmodified or ‘pass-through’ channels. The pass-through channels are used for safety-of-flight monitoring of critical blade and hub structural components. Amplification of the data channels results in enhanced transducer signal-to-noise ratios before entering the slipring. The entire RAS system is contained in a cylindrical housing 7.0 inches in diameter and 5.6 inches in height and air-cooled. The RAS cylindrical housing is divided into 16 ‘pie’ shaped modules each containing 16-hybrid amplifier cards. The RAS design utilizes hybrid circuitry which minimizes the size of each amplifier card. Each card has four selectable gain and three selectable

calibration resistors. The gain and resistance settings are programmable via an RS 232 link to a PC.

Slip-Ring Assembly
A 300-channel slipring on the right rotor system transmits measurements into the non-rotating frame. The slipring is submerged in a re-circulating coolant. The left hand rotor has a standard 100-channel slipring.

Gimbaled Hub
The TRAM baseline gimbaled rotor hub incorporates a constant velocity joint (spherical bearing and elastomeric torque links) and is dynamically and kinematically similar to the V-22 aircraft. The rotor control system is comprised of three electromechanical actuators, a rise-and-fall swashplate, and rotating and non-rotating scissors allowing full rotor collective and cyclic control. The rotor hub assembly transfers the loads from the flexbeam into the stub shaft. The hub is free to gimbal 8 degrees about the hemispherical retainers before contacting a rubber bumper. The elastomeric design of the three torque links allows the torque to be transferred from the gimbal hub to the non-gimbaling torque link hub. Figure 9 is a schematic of the TRAM hub.

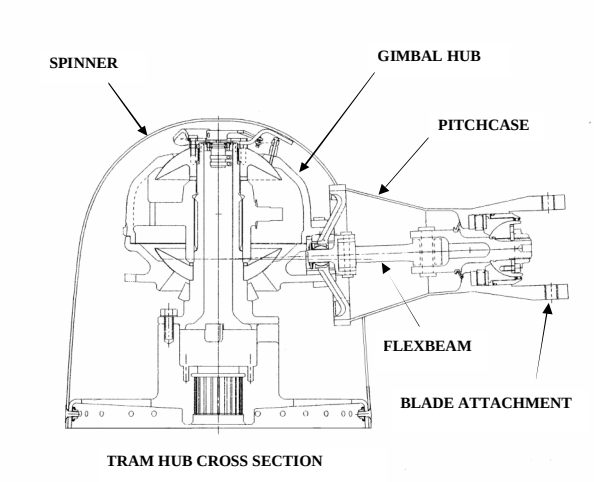

Figure 9. TRAM Hub Assembly

Blade Assembly
The TRAM blade assembly consists of the rotor blade, the pitchcase with blade attachment, and the flexbeam. All forces and moments at the root of the rotor blade are transferred through its rigid attachment to the pitchcase/blade-grip subassembly. The outboard centering bearing (between the pitchcase and the outboard end of the flexbeam) allows only the centrifugal force and flapwise and chordwise shears to be transferred to the flexbeam. The flexbeam and pitchcase serve as dual load paths for the shears, while the torsion, flapwise, and chordwise moments are carried exclusively by the pitchcase. The inboard centering bearing transfers the pitchcase shears back into the flexbeam. The resultant loads in the flexbeam are transferred to the rotor hub through a rigid connection. Blade pitch control moments are applied to the pitchcase through a conventional pitch arm, control rod, and swashplate assembly.

Blade Construction
The FS TRAM 1/4-scale V-22 rotor diameter is 9.5 feet with a thrust-weighted solidity of 0.105. All blades have the same mass distribution properties and high fidelity airfoil contours. The blade first elastic modes (flapwise, chordwise, and torsional) are dynamically scaled to V-22 frequencies. The structural design of the TRAM blades is based on a glass/graphite epoxy hybrid composite. The blade consists of pre-cured spar and skin/core joined assemblies. Instrumentation wiring packages are surface mounted into recessed cavities on the blade skin for measuring pressure or strain. The primary structural element of the blade is a hollow spar. Blade loads are transferred through the rectangular box beam spar structure to the root end lugs using spar caps. Section balance at the blade tip is provided by a cast leading edge weight made of an epoxy resin and tungsten mixture with a tungsten rod molded into the core. The afterbody is a thin skin sandwich structure. A machined aluminum tip fitting is integrated into the spar structure to produce the chordwise CG offsets required in the scaled V-22 blade tip. Spanwise and chordwise balance capabilities are adjusted by installing tungsten rods cut to the length required to obtain the proper blade balance condition. The tip fitting is bonded to the outer torque wrap of the spar assembly.

Rotor Blade Instrumentation
The TRAM blade inventory consists of both pressure and strain-gauged instrumented blades. Pressure-instrumented blades were not used in this entry, but are mentioned here to provide a comprehensive description of the model capabilities for future testing. Each strain-gauged blade was fabricated with 14 strain gauge (full-bending) bridges installed: five flapwise bending-moment, five chordwise bending-moment, and four torsion. There are 149 pressure transducers evenly distributed over two right-hand rotor blades. Chordwise rows of pressure transducers have been distributed between two blades in a manner that minimizes the difference in span moment due to mass distribution effects of the instrumentation wiring. The transducers are flush-mounted with a pressure range of 25 psi absolute. Three transducer model types were installed: pipette, B-screen, and flatpack. All transducer types have the same electrical specifications with a flat-response characteristic of less than 0.5 dB out to 60 kHz. References 5 and 8 describe the pressure blades, pressure data acquisition, and blade airloads data obtained in the TRAM/DNW test.

There was one active strain-gauged blade on each rotor during all testing. (There are three available strain-gauged blades for each side, but only one per side can be electrically connected at a time.) The gauge sensitivities for each strain-gauged blade vary and the sensitivities are

verified at the time the blade is installed on the model. All strain gauge data were acquired at 64 samples per revolution. The left and right safety-of-flight (SOF) blades have the same instrumentation, however, five gauges on the left side were inactive due to the limited number of slipring channels.

Rotor Balances

The Full-Span TRAM has two six-component strain-gauged rotor balances, one in each nacelle just below the hub, with a fail-safe retention design. The non-rotating rotor balances are instrumented with primary and backup sets of gauges, which allow the measurement of the rotor aerodynamic forces and moments. A flexible shaft-coupling provides transmission of torque to the rotor hub through a load path independent of the rotor balance. This coupling is instrumented to measure torque and any residual thrust carried by the drive system. The rotor balance maximum design loads are provided in Table 1. The roll and pitch shown in Table 1 are the design loads at the rotor hub. The balance moment loading is 18,000 in-lbs and accounts for the extra moment generated by a side/drag force at the hub which is approximately 18 inches above the balance moment center.

Table 1. Rotor balance design hub load limits

Measurement	Design Limit
Thrust Force	+3000, -500 lbs.
Side Force	± 750 lbs.
Drag Force	± 750 lbs.
Pitch Moment	± 2400 in-lbs.
Roll Moment	± 2400 in-lbs.
Yaw Moment	N/A
Torque*	+15,600 in-lbs.

*Torque measured by flex-coupling, rotor balance yaw moment is considered residual torque.

A heater system is integrated into each rotor balance. Heater coils on the balance are close-loop controlled to maintain constant balance temperature during data acquisition. Each flexure has eight thermocouples installed to record the rotor balance distributed temperature characteristics during a run. The base of the rotor balance is mounted to the nacelle transmission on the non-metric side and the static mast is mounted to the metric side of the balance. The rotor balance is mounted in the nacelle with ceramic insulators on both the metric and non-metric sides to minimize the heat transfer to the balance from the transmission and the static mast.

Fuselage Balance

The fuselage balance is located inside the pedestal located below the attachment points of the spars to the fuselage. The combined loads of the wing, rotors, fuselage and empennage are carried through the fuselage body structure to the balance where strain gauge measurements are taken. The centroid of the fuselage balance is located 1.0" aft of the angle of attack rotation axis. No provisions were made to maintain a constant temperature at the fuselage balance and some temperature related variations in balance gauge responses were seen in this entry. (Fuselage data quality is discussed further in the results section.) The fuselage balance maximum design loads are provided in Table 2.

Table 2. FS TRAM fuselage balance design limits.

	Design Limit
Normal Force	+4000, -8500 lbs.
Side Force	±1500 lbs.
Drag Force	+2000, -6000 lbs.
Pitch Moment	+100,000, -150,000 in-lbs.
Roll Moment	± 35,000 in-lbs.
Yaw Moment	±40,000 in-lbs.

Wing Pressures

The FS TRAM has 185 static pressure ports distributed across the left hand wing and flaperons in 5 span-wise locations. These measurements are used to study wing lift and rotor download in hover and forward flight. Data are acquired on an independent PC running an in-house LabVIEW program with a 3-Hz low-pass filter. Reference 15 describes the wing pressure set up, acquisition and results.

MODEL DEVELOPMENT AND CHECK-OUT

Over 700 research, health monitoring, and SOF instrumentation channels are incorporated into the FS TRAM. The health of these gauges, checkloading the components, and the review of the system as a whole is required before testing can begin. This section discusses some of the analysis and checks conducted on the FS TRAM.

Offset Shifts

Routine instrumentation checks (Zero, resistance calibration (Rcal), and Static points) are performed at the beginning and end of every run with no rotation, no wind, all utility power on, and the model in a standard configuration. Prior to each run, all instrumentation voltages are zeroed out and a Zero-point is acquired. The starting Zero point data are used for zero-subtraction in the data reduction equations. An ending Zero point is acquired to check for instrumentation drift during the run. The Rcal points are taken with a known shunt resistor applied to the sensor, causing a forced voltage input into the system, resulting in a derived EU-response (somewhere between 60% to 100% of the Engineering Unit limits). These Rcal data are used in sensitivity adjustments for selected channels. Static data points are taken with all channels set for normal data acquisition. The Zeros, Rcals and Static data points are reviewed to check for channel health. A simulated rotor RPM signal (1555) is used for data points acquired with the rotor

stopped, since all data acquisition is synchronized to the rotor.

EMI Noise

An item of particular concern at the beginning of this test was the possibility of electro-magnetic interference (EMI) from the electric drive motors. These motors have a switching frequency of 10,000 Hz and a waveform frequency equal to motor RPM divided by 12. The analog output of the safety-of-flight signal conditioners, both filtered and unfiltered, were examined with an HP signal analyzer during a series of balancing runs. No measurable trace of the motor switching frequency was found and the levels of the waveform frequencies were never above the ten millivolt level on any channel even in the unfiltered signal. The four pole Bessel filters are set to 600 Hz cutoff frequency which corresponds to a motor RPM of 7200. Only one research data point was acquired at a lower RPM. Measurements in that data point were examined and no trace of EMI was found.

Aliasing

Data were acquired at 64 samples per rotor revolution for 32 revolutions with a nominal RPM of 1413 corresponding to 1507 samples per second. Aliasing occurs as a reflection around half of the sampling rate so minimal aliasing should occur for sampling frequencies above twice the cutoff of the amplifier filters. The research data were taken at sampling frequencies above 1400 Hz to prevent aliasing.

Fuselage Balance Temperature Drifts

Beginning and ending static points were reviewed to assess drifts on the fuselage balance measurements. This drift was traced to changes in the average temperature of the balance throughout the run and to temperature differentials within the balance itself. Unlike the rotor balances, which contain heaters to maintain a constant temperature, the fuselage balance had no provisions to enforce a constant temperature, nor was any insulation used between the balance and nearby high temperature components. Fuselage balance measurements suffered significant drifts as a result. This is discussed later in the paper but mentioned here because instrumentation checks flagged the problem.

Static Checks

Figure 10 shows the FS TRAM being lifted into the test section. After the FS TRAM was installed in the test section, extensive build-up was required to connect and verify power, utilities, controls, and instrumentation. Every connection was checked for proper installation and electrical response. Each transducer was physically loaded whenever possible in an end-to-end check through the data acquisition system to check for proper sign and magnitude response. The check examined instrumentation and software set up for the correct sign convention and magnitude of raw and derived parameters with respect to static applied loads. Balance response was recorded under a number of load conditions including changing the fuselage angle of attack, rotating the rotor shaft, applying loading to the left- and right-hand rotor balance using dummy hubs, applying loading to the rotor balance using a cross-beam calibration fixture, and applying loads to the wing spars using a spreader bar. The applied check loading on each TRAM balance is computed from the load cell data and the load vector orientation and is reviewed in the form of the three forces (normal, axial and side force) and three moments (pitching, rolling, and yawing moment) on the subject balance.

Figure 10. The TRAM is lifted into the 40-by 80-Foot Wind Tunnel Test Section. Clamshell doors are shown partially open.

DATA ACQUISITION

The principle data acquisition system used for the TRAM is the NASA NPRIME system. This system was used to acquire all model parameters, acoustic measurements and some tunnel parameters. The data acquisition portion of NPRIME consists of a series of VME boxes, called AFEDS, each capable of acquiring a wide range of channels and data rates. Each box consists of a control computer, RAM memory for temporary data storage, a high-speed data network card and several analog-to-digital converter cards. Each box is connected to a central controller which synchronizes data acquisition to an external trigger. For the TRAM test, the AFEDS are divided into high-speed data boxes (for blade pressures and acoustics) and low-speed data boxes. There were 4 high-speed AFEDS which were available to acquire the 167 data channels at a rate of 2048 samples per rev. There are 3 low-speed AFEDS which were used to acquire the model parameters including rotor balance channels, rotor blade strain gauges and control system loads. These are acquired at a rate of 64 samples per rev for 32 revolutions. For a typical run at Mtip = 0.63, RPM = 1413, the sample rate is 1507 and a low pass filter of 600 Hz is used. Acoustic data were acquired at 2048 samples per rev for 48K samples per second and a low-pass filter of 20Khz. The wing pressure data acquisition

system and the safety of flight monitoring systems were independent of NPRIME.

BALANCE DATA REDUCTION

There are three balances on the FS TRAM; a right and left rotor balance, and a fuselage balance. Balance load measurements are required for safety of flight monitoring, setting the test condition, and performance measurements. Each balance has multiple strain gauges allowing for the determination of the three force and three moment loading in the non-rotating balance axis system. The rotating instrumented shaft flex-coupling measures torque and residual thrust in the shaft. The rotor balance load data and shaft flex-coupling load measurements are combined into the three forces and three moments (3F/3M) representing the rotor loading. Redundant gauges are installed on all balances and shaft flex-couplings. The load measurements from the two gauge sets are identified as L1 and L2 for the left rotor balance and R1, R2 for the right rotor balance and F1 and F2 for the fuselage balance.

Tares

Tare data are taken to compensate or correct for gravity and hub aerodynamic interferences. The tare data are subtracted from the acquired research data to isolate the measurements of interest. The effect of gravity, or weight tare, on each balance can be acquired with the hubs rotating or not rotating and is a function of fuselage angle of attack and nacelle angle. Since weight tares are dependent on model arrangement and nacelle orientation, a fuselage angle of attack sweep took place for every model configuration. The effect of hub aerodynamics is determined by acquiring balance data without the rotor blades installed. Such data, or aerotares, were acquired with hub rotation and without blades at several tunnel speeds. Aerotares are dependent on tunnel velocity, fuselage angle and nacelle angle. Rotor balance data in forward flight are corrected for weight tare and aerotare.

BALANCE DATA QUALITY REVIEW

Individual balance parameters are reviewed for each run. Data from each rotor, as well as the two redundant balance gauge sets, should exhibit the same load magnitude and trend under each test condition. Dead or inconsistent channels are identified. There were several instrumentation channels that became impaired during this test, and the redundant balance gauges allowed continued measurement of rotor loading. Another means to check the quality of the gauges is to examine the starting and ending static points. As an example of checking data quality, data from hover Run 189 is shown in this section. The model was pitched nose down at –9 deg and the test section overhead clamshell doors were fully open to prevent re-circulation. The flaperons were set to 70 deg, (trailing edge down), and the elevator and rudders were at zero deg. The rotor balance heaters were on, and all fairings except the nacelle fairings were installed. Beginning and ending static points for the three forces for run 189 are shown in Figures 11 through 13. Ideally, all gauges should read zero at both points, but this deviation (< 10 lbs) was typical. Much larger deviations, sometimes on the order of 100 lbs, were seen when the rotor balance heaters were off.

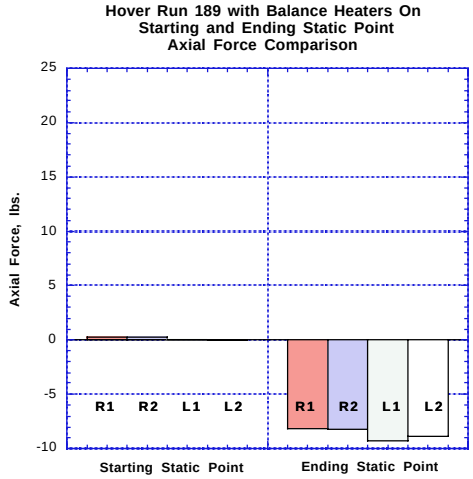

Figure 11. Starting and ending static data for Axial Force for Run 189.

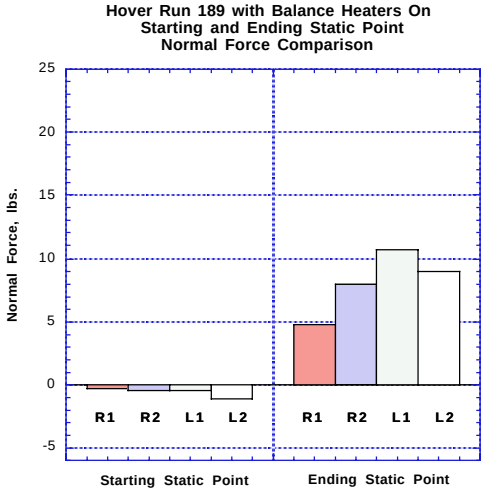

Figure 12. Starting and ending static data for Normal Force for Run 189.

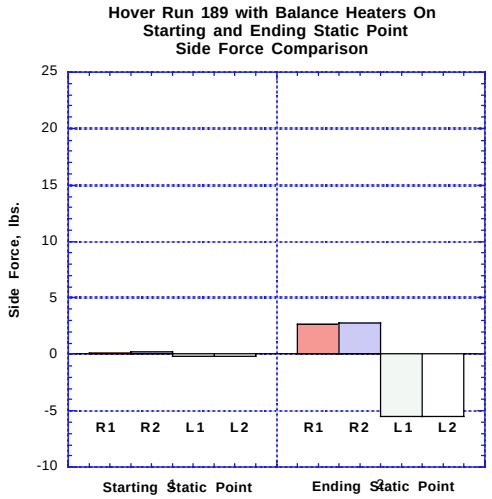

Figure 13. Starting and ending static data for Side Force for Run 189.

Differences were seen between left and right rotor during Run 189. Figure 14 below investigates the rotor normal force response as a function of rotor collective. The left rotor appears to have less response for the same input, although the slopes of the lines are close. The differences could be caused by a physical difference between the two rotor sets, a variation of inflow in the two rotor discs, the accuracy of the blade pitch setting, or the collective or normal force measurements. The two rotors are considered separate data sets and are always shown independently unless their differences are indiscernible.

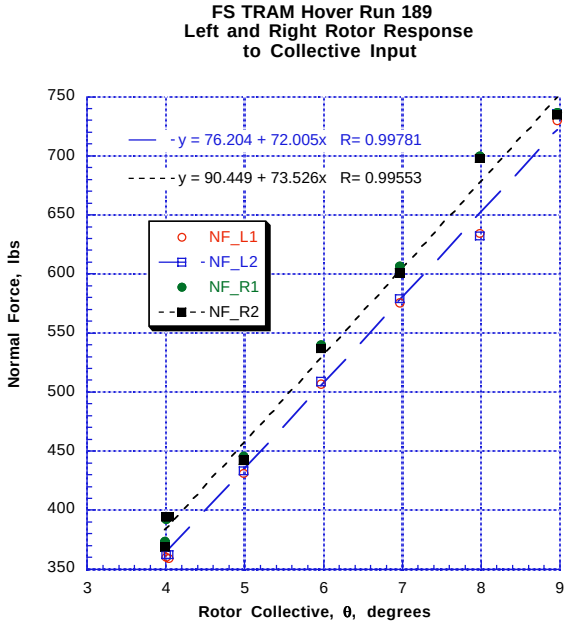

Figure 14. Left and Right Rotor Response to Collective Input.

Figure 15 shows the thrust and power coefficients for Run 189, except for R1 data due to a bad FCTQ gauge. Typical of all the data, some scatter is seen but magnitudes and trends are similar for left and right, gauges 1 and 2.

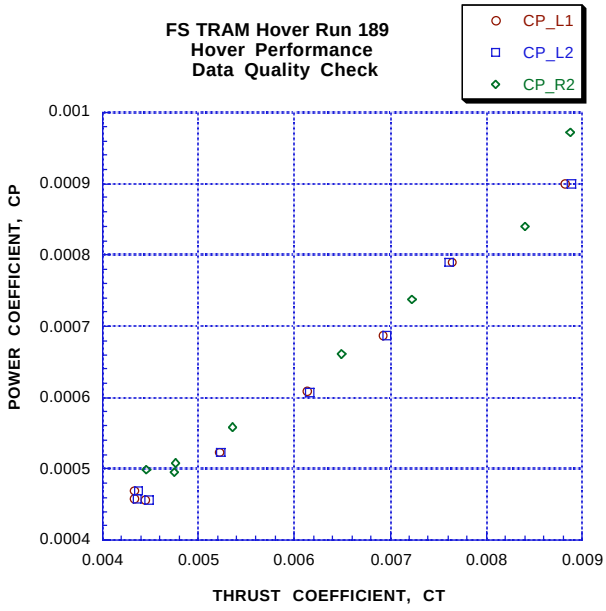

Figure 15. FS TRAM Hover Performance Data for Run 189.

PERFORMANCE RESULTS

Limited research data were acquired for the FS TRAM in the 40- by 80-Foot Wind Tunnel. Rotor performance measurements were taken on the FS TRAM during hover, helicopter-mode forward flight, and airframe aerodynamic runs. All the FS TRAM data were acquired at a hover tip Mach number of 0.63 in order to match the TRAM/DNW data taken at that condition due to motor limitations. The FS TRAM motors are capable of providing an Mtip equal to 0.708, corresponding to a nominal 1588 rotor RPM, but since the test ended prematurely, data at higher RPMs were not obtained. Also, desired repeat points of critical research data could not be obtained due to early test termination.

The basic wind tunnel testing procedure with the FS TRAM was to take Zero, Rcal, and Static points, begin rotation at 4 deg blade pitch, set up on a given angle of attack, advance ratio, and thrust while trimming the rotor to zero flapping.

Research quality hover data were obtained during two runs; 189 and 191. For these runs, the fuselage angle of attack was -9 deg, and the test section clamshell doors were open. The nose down attitude of the fuselage blows the wake down the test section into the diffuser and the open overhead doors expand the top of the test section into a larger high-bay area which also helps to reduce re-circulation. Figure 10, (shown previously), shows the

test section overhead clamshell doors partially open. The TRAM nacelles were set at 90 deg (helicopter mode) and the rotor balance heaters were on to maintain the balance at constant temperature. In hover, certain rotor hub components would tend to overheat restricting run duration. The nacelle fairings were removed to enable continuous hover data runs. The effect of the missing nacelle fairings on rotor performance has not yet been quantified but is believed to be within the scatter of the data. The SOF blades were rotating at Mtip = 0.63, wing flaperons were 70 deg down, and trim was set to minimize blade flapping. Collective sweeps were performed.

In some cases, one gauge may be bad and therefore not shown, or the data from both gauge sets are so similar, only loading from one set are shown for clarity. Only one gauge set loading on one rotor is occasionally used if it is representative of all other rotor load data. Figure 16 shows the FS TRAM hover Figure of Merit (FM) as a function of thrust coefficient over rotor solidity (CT/σ). Figure 17 shows the power coefficient (CP) plotted against the thrust coefficient (CT). Figure 18 presents the thrust coefficient (CT) as a function of rotor collective measured at the 3/4 blade radius.

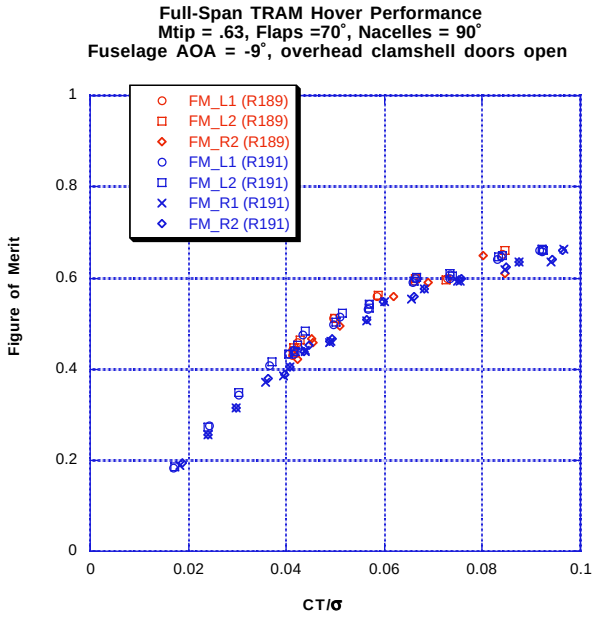

Figure 16. Full-Span TRAM Hover Figure of Merit

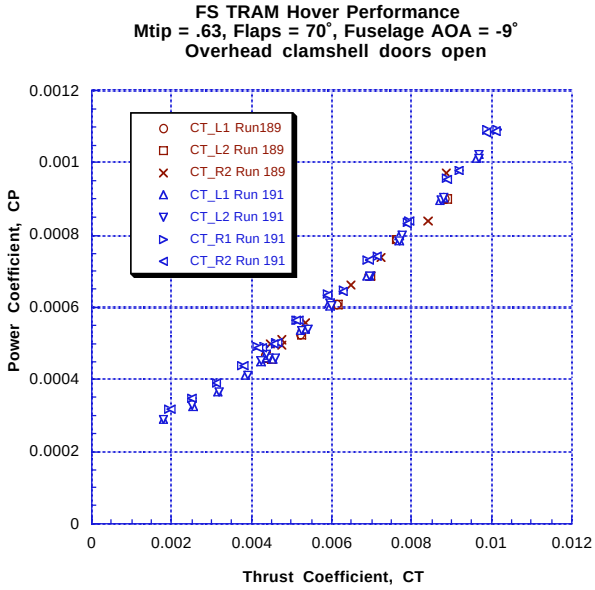

Figure 17. Full-Span TRAM Thrust and Power coefficient.

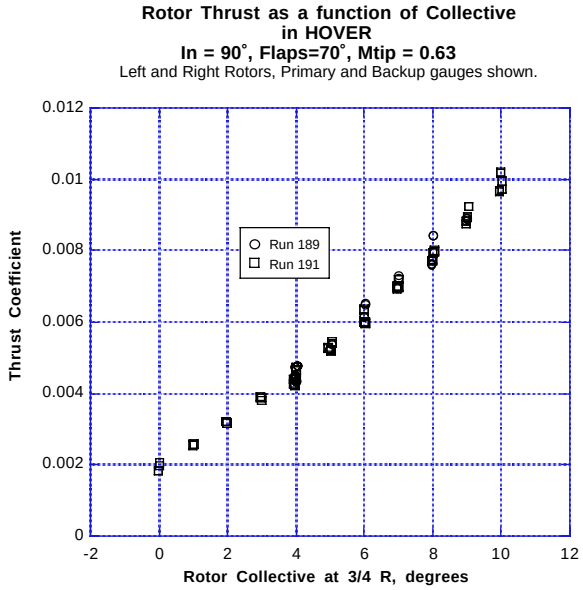

Figure 18. Full-Span TRAM Thrust and Collective

Figure 19 shows the power coefficient, CP, as a function of rotor collective at the 3/4 blade radius. There is scatter between the rotors, gauge sets, and runs, but the general trends are clear.

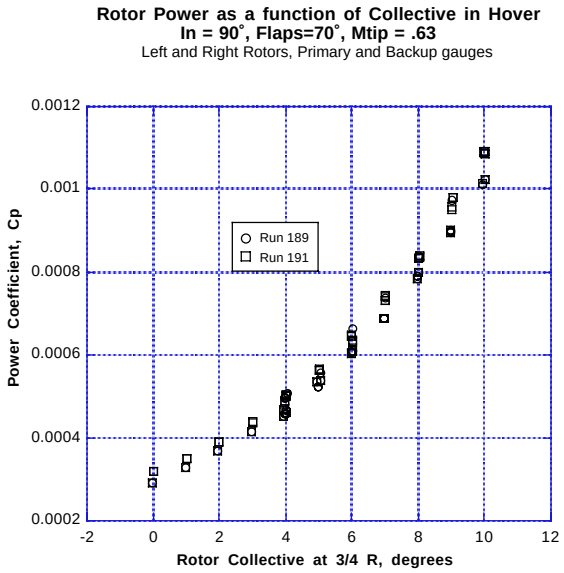

Figure 19. Full Span TRAM Power and Collective

Figure 20 presents CT to the 3/2 power as a function of CP for the each gauge set. Blade element theory gives CP as a function of solidity (σ), thrust coefficient (CT), section drag coefficient, (c_d) and κ, where κ is the ratio of induced power to momentum theory (Ref. 16). (It is noted that for tiltrotors, minimum power is not necessarily at zero thrust and c_d and κ can vary significantly with thrust, even without considering stall.) Using the blade element theory, the slope and intercept for R2 data in Figure 20, for example, gives a mean drag coefficient of .0183, and an induced efficiency factor of κ equal to 1.181.

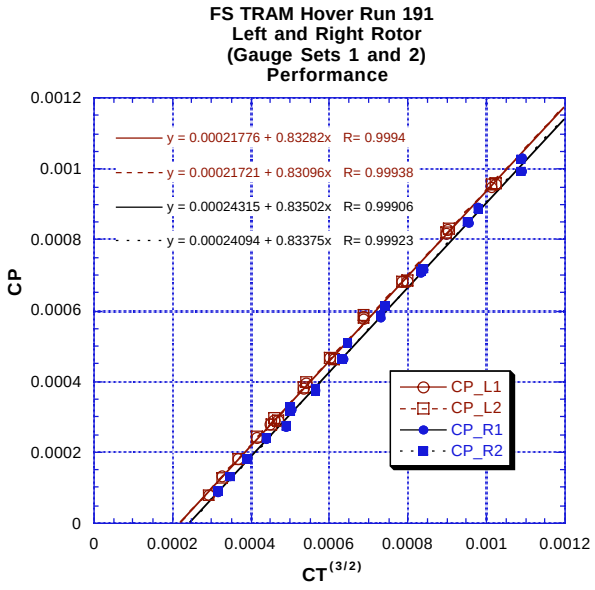

Figure 20. Full Span TRAM linear relation between thrust and power coefficients.

Four sets of test data are presented and compared to this Full-Span TRAM test. The Boeing Vertol Wing Tunnel (BVWT) 319 test was a 0.15-scale full-span model (Ref. 17), the Bell Helicopter Textron Inc. (BHTI) was a 0.15-scale semi-span model (Ref. 18), the Outdoor Aerodynamic Research Facility (OARF) test was a 2/3 scale JVX isolated rotor (Ref. 19), and the TRAM/DNW test used the isolated TRAM rotor (Ref. 8). Table 3 lists the model scale, rotor radius (R), rotor thrust-weighted solidity (σ), hover tip velocity (Vtip), and Reynolds number (Re), for the four tests. Figure 21 shows the FS TRAM hover performance in terms of power and thrust coefficients over solidity compared to other tiltrotor model test data at similar conditions.

Table 3. Properties of Tiltrotor Model Tests.

Rotor	Scale	R (ft)	σ	Vtip (fps)	Re (x 10^6)
JVX	0.658	12.5	0.1138	760	5.400
TRAM	0.25	4.75	0.105	705	1.756
BHTI	0.15	2.85	0.105	789.5	1.180
BVWT	0.15	2.85	0.1138	789.5	1.279

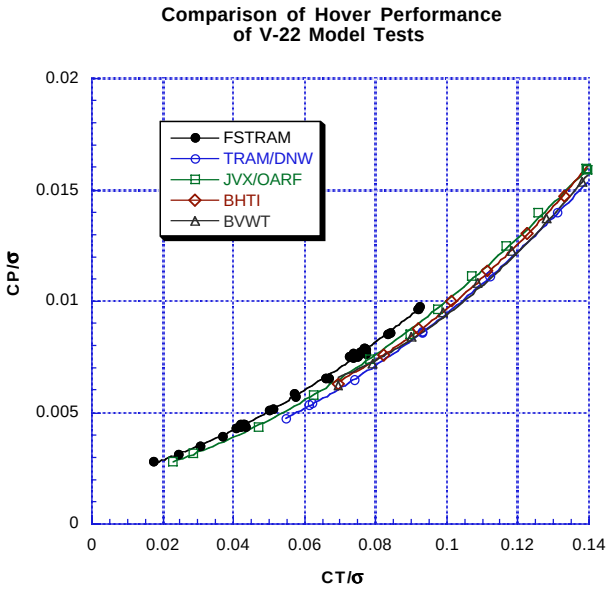

Figure 21. FS TRAM Hover Performance compared to other tiltrotor data at similar conditions.

Simple Reynolds number and solidity corrections were made to the model test data to compare the results with respect to V-22 full-scale performance. The correction approach is described in Appendix A. Reference 2 0 discusses some of the scaling issues when comparing wind tunnel model and full-scale rotor performance. Figure 22 shows the hover Figure of Merit for each of the tests with the Reynolds number and solidity corrections included. The data suggests reduced rotor performance for the full-span models as compared to isolated and semi-span models.

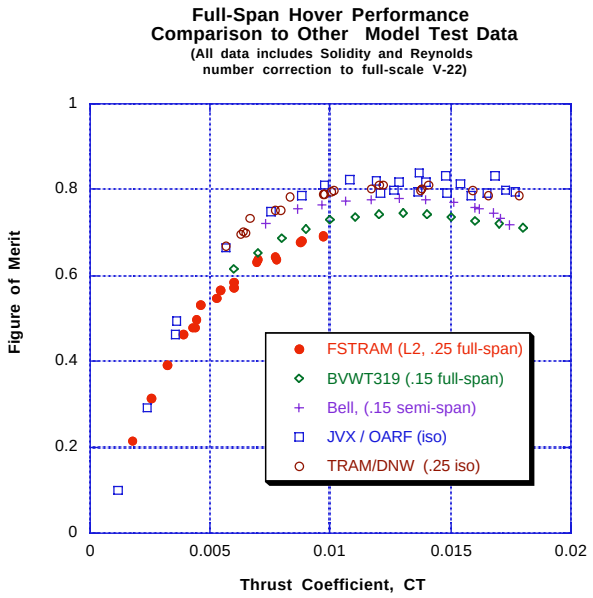

Figure 22. FS TRAM hover performance comparison to other model test data, including Reynolds Number Corrections.

Two forward flight runs were performed in helicopter mode at nacelle angle of 85 deg. Thrust sweeps were performed at advance ratios of 0.10 and 0.15 for rotor shaft angle of +6 deg at Mtip = 0.63 (Run 201). Rotor balance heaters were set at 120 deg and all fairings were on. Figure 23 is the thrust and power coefficients over rotor solidity for the two advance ratios.

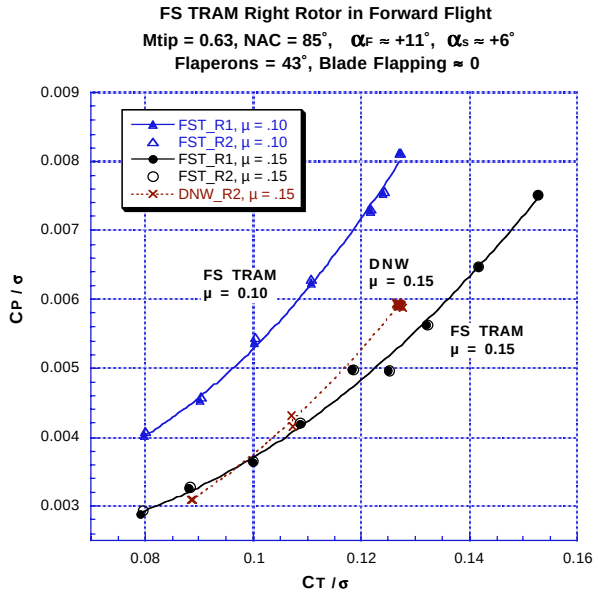

Figure 23. TRAM Right Rotor performance data in Helicopter mode forward flight.

ADDITIONAL RESULTS

The primary focus of this paper has been an overview of the model and review of balance data, but significant other data were obtained. This section briefly describes measurements acquired and presents example data.

Acoustic Data

One objective of the FS TRAM test was to acquire acoustic measurements similar to those acquired at the DNW to help validate NASA's tiltrotor aeroacoustic prediction code, TRAC, described in Reference 21. Blade vortex interaction (BVI) noise directivity measurements were acquired during forward flight Run 201, although no complete traverse sweeps were performed. The acoustic measurements were made using twelve microphones mounted on a dual traverse system. The microphones traversed in a plane beneath the rotors with emphasis on capturing the advancing side BVI noise of the right hand rotor. The microphone signals were acquired simultaneously with blade structural loads and rotor performance. The wings are placed 16.6 feet (1.75 rotor diameters) below the plane of the rotors when the FS TRAM is in the reference position (i.e., fuselage angle of attack at +5 deg, nacelle angle at 85 deg). Each wing carries 6 microphones spaced 26.6 inches apart. There were 16 streamwise locations on the West (starboard) side and 9 streamwise locations on the East (port) side, spaced 40 inches apart. The rails were covered with 2-inch thick foam to minimize noise reflections. Foam was also glued to the FS TRAM main strut, bayonet strut and transition fairings. Background noise data were acquired during aerotare runs and a reflection test was performed to examine the model and facility acoustic environment. Microphone calibrations were performed daily using a 124dB, 250Hz pistonphone.

Laser Light Sheet Data

Wake geometry measurements were taken to study the development and structure of a dual vortex system generated during BVI conditions. Laser Light Sheet (LLS) images were obtained in the 40- by 80-Foot Wind Tunnel using a super VHS digital video recorder. Results will be compared to images obtained from the TRAM/DNW isolated rotor test, described in Reference 4. Data were obtained for two thrust levels, CT=.009 and .013, for advance ratios 0.10 and 0.15. Figure 24 is a sample LLS flow visualization image showing a counter-rotating vortex pair.

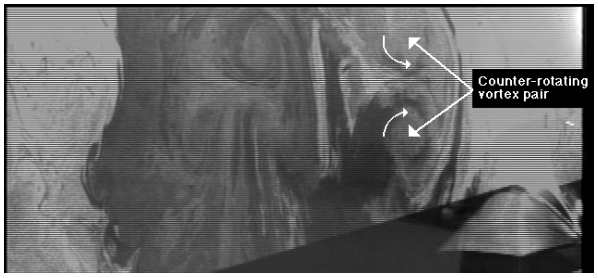

Figure 24. Sample LLS flow visualization image, μ = 0.15, CT = .009, Mtip = 0.63, αs = +6.

Airframe Aerodynamic Runs

Airframe aerodynamic runs were performed with rotors off, clean spinners and all fairings installed. Angle of attack sweeps were performed at 42, 63, 84 and 104 knots for 60 and 85 degree nacelle angles with flaperons set to 43 deg (Runs 206 and 207). Run 208 was an alpha sweep at 84 knots with the flaperons at 70 deg. Twelve points were taken at the same condition to check repeatability (63 knots, Ashaft = 6 deg, flaps 43) while PIV seeding and software were tested (also Run 208). Elevator sweeps were performed at 104 and 150 knots. Angle of attack sweeps were performed at 200 knots for elevator angles of -17, -10, 0, 5, and 7 deg Runs 209 and 210). (TRAM negative elevator angle is trailing edge down.) Lastly, small angle of attack sweeps were performed with the elevator at -17 deg (t.e. down) for 250 and 290 knots (Run 211). This data will be reviewed once fuselage balance data issues are clarified.

Fuselage Balance Temperature Corrections

Initial checks of fuselage balance data showed significant drift and was traced to temperature variations across the balance and over time. A first order temperature correction was calculated using limited data acquired during a checkout run that had several repeat points over time. Linear curve-fits were computed for each of the eight equivalent calibration voltage measurements on the fuselage balance against a local flexure temperature gauge. The correction reduced data scatter and improved magnitude results. During run 206, for example, the fuselage balance increased in temperature throughout the run. Figure 25 is the Drag Polar data from that run (CA or CD vs. CL). Significant scatter is evident in the data. Figure 26 is the same data with the temperature correction applied. Slight improvement is seen with better matching of primary and secondary gauges and better correlation between the different velocities.

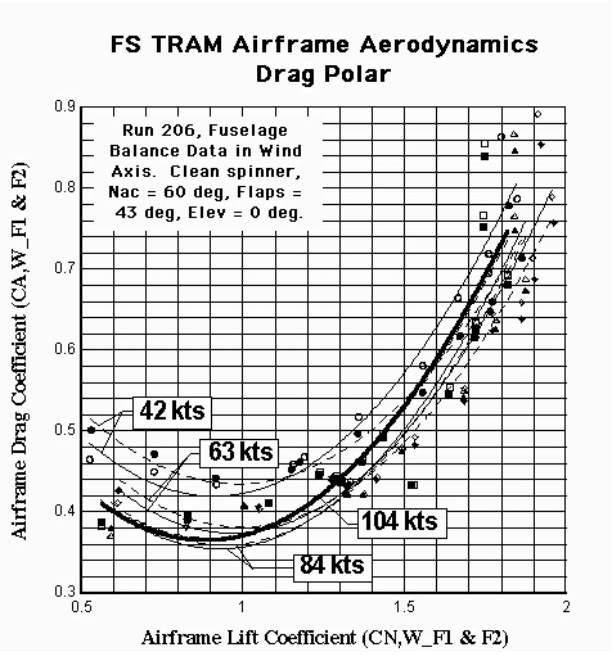

Figure 25. Sample Drag Polar. (Plot courtesy of T. Trept, Bell Helicopters)

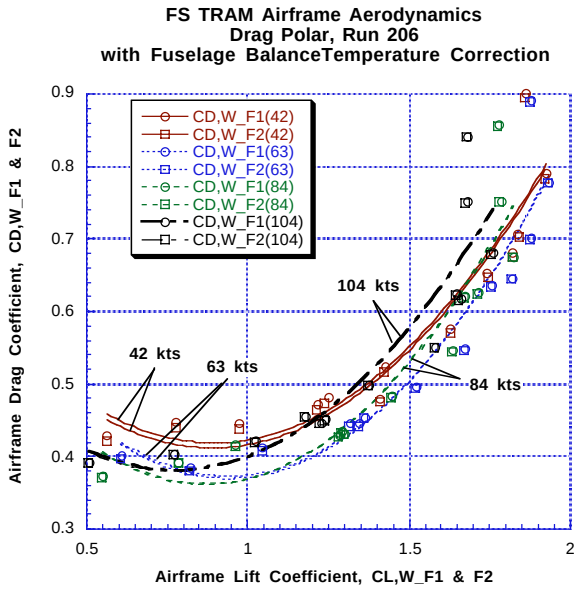

Figure 26. Drag Polar after fuselage balance correction.

In some cases, the magnitude improvement was significant. In a hover flaperon sweep, shown if Figure 27, initial data incorrectly showed the fuselage force being greater than the combined rotor forces (negative download). Corrected data showed a more reasonable download, but did not improve the repeatability for a given flap angle, i.e. 70 deg. Also, a minimum download bucket is not seen. Repeat data were not obtained.

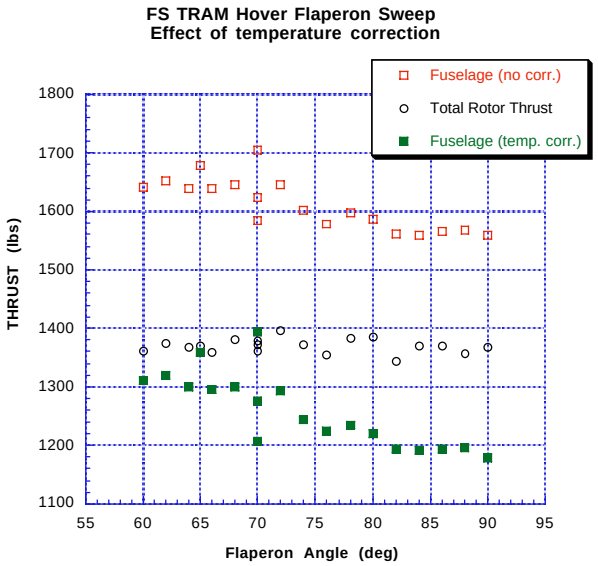

Figure 27. Fuselage response to flaperon sweep with and without temperature correction.

Options are being investigated to minimize the temperature changes on the fuselage balance during operations. Additional data will be acquired to improve the correction method.

Wing Pressure Data

Wing pressure measurements were acquired from 185 static pressure taps installed on the left-hand wing and flap of the FS TRAM. Static Pressure data were acquired throughout the test for investigation of rotor-on-wing interactions in hover, wing download and rotor-on-wing interactions in helicopter-mode forward-flight. Wing pressure distributions were obtained for wing airloads (rotor-off only) in transition and airplane-mode forward-flight. Figure 28 is a sample of wing static pressure data obtained in hover. Reference 15 provides a comprehensive presentation and discussion of the static pressure data results from this FS TRAM test.

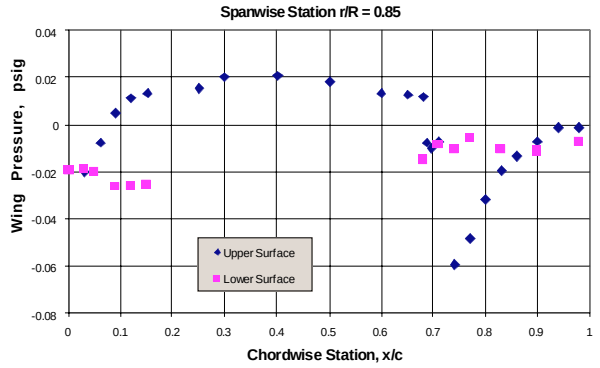

Figure 28. Sample wing pressure data for FS TRAM in Hover.

Left and Right Strain-Gauged Blades

The FS TRAM underwent extensive developmental testing prior to the wind tunnel program. Many motor, rotor, and drivetrain balancing runs were performed. Safety-of-flight (SOF) structural gauges were monitored to ensure safe operations within performance limits. There are strain gauges on the SOF blades that measure flap and chordwise bending, and torsion. These loads are required during flight to monitor the health of the blades. Additionally, since the blades are dynamically scaled, the structural data can be used for blade dynamic research and validation of comprehensive codes such as CAMRAD II (Ref. 22). Figure 29 is an example of mean blade flapping data where the numbers shown in the legend refer to the gauge location on the blade (i.e. BLFB365 is blade flap bending moment at 36.5% rotor radius. An example of pitch-link loads (A, B, or C referring to position on the hub) is shown in Figure 30.

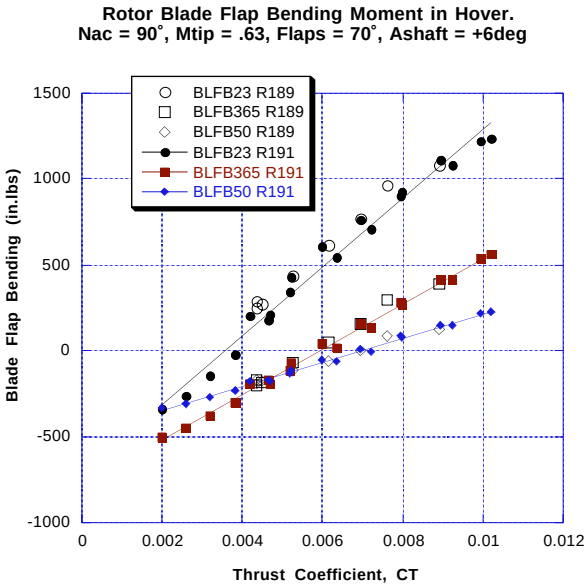

Figure 29. Mean flap bending moment for hover runs 189 and 191.

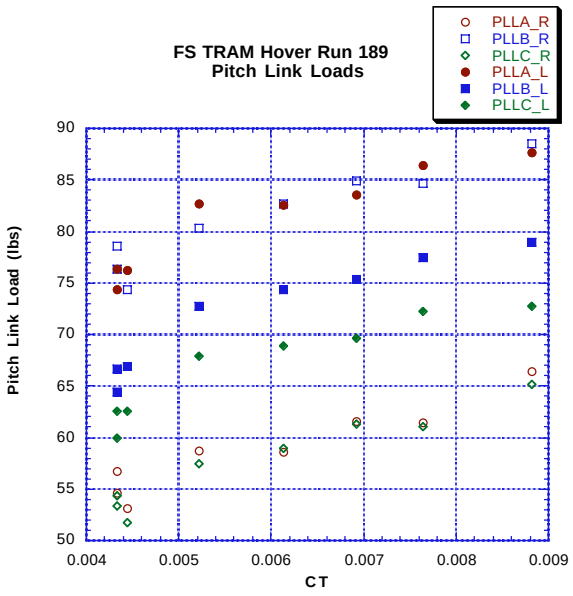

Figure 30. FS TRAM Mean Pitch Link Loads in Hover.

RECOMMENDATIONS FOR FUTURE TESTING

The Full-Span TRAM initial testing overcame loss of rotor balance gauges and lack of repeatability of fuselage balance results due to temperature variations. Redundant gauges on the rotor balances allowed for continuation of the test. The lost gauges are to be repaired to allow the next test phase to start with fully redundant rotor balance gauge sets. Fuselage balance drift due to temperature was partly mitigated by using a simple correction method described in this paper. Thermal isolation is recommended for future testing and additional data can be acquired to improve the correction method. Premature conclusion of the test limited the acquisition of desired repeat points. Future testing will include multiple repeat points and parametric sweeps of critical research data.

CONCLUDING REMARKS

A full-span powered tiltrotor model was developed and introductory wind tunnel testing was completed. Full-Span TRAM construction, instrumentation and measurement capabilities were described. Significant experience was gained in the operation of the model during this initial check-out phase. Valuable research data were obtained such as rotor performance data in the presence of a second rotor, wing and fuselage, and acoustic and wing pressure data with and without rotor blades operating. Rotor wake measurements using the laser light sheet technique were successfully acquired in the 40- by 80-foot wind tunnel. The long-term objectives of the FS TRAM are to acquire and document a comprehensive tiltrotor database, and provide a platform for testing future proprotor designs. The experimental data can be used for development and validation of prediction and simulation codes, as well as supplementing flight test data.

ACKNOWLEDGEMENTS

The Full-Span TRAM development and testing was supported by the NASA Short Haul Civil Tiltrotor (SHCT) Project, the NASA Rotorcraft Research and Technology Base Program, and the U.S. Army Aeroflightdynamics Directorate (AFDD). The authors wish to acknowledge the entire TRAM test team, shown in Figure 31, whose dedication and perseverance made the program possible. Special thanks to the following people who provided data, graphics, or other valuable input for this paper: Michael (Tony) McVeigh and Robert Mayer (Boeing); Ted Trept, Mike Farrell, and Tom Wood (Bell); Steve Woods (NAVAIR); Wayne Johnson and Gloria Yamauchi (NASA Ames); Jan van Aken (Aerospace Computing, Inc.); Jeff Kwong (UCLA); and Michael Heffner.

Figure 31. The NASA Ames Research Center FS TRAM 40- by 80-Foot Wind Tunnel Test Team.

REFERENCES

1. Young, L. A., Booth, E. R., Yamauchi, G. K., Botha, G., Dawson, S., "Overview of the Testing of a Small-Scale Proprotor," American Helicopter Society 55th Annual Forum, Montreal, Canada, May 1999.

2. Young, L. A., "Tilt Rotor Aeroacoustic Model (TRAM): A New Rotorcraft Research Facility," American Helicopter Society International Specialist's Meeting on Advanced Rotorcraft

Technology and Disaster Relief, Gifu, Japan, April 1998.

3. Johnson, J. L. and Young, L. A., "Tilt Rotor Aeroacoustic Model Project," Confederation of European Aerospace Societies (CEAS) Forum on Aeroacoustics of Rotors and Propellers, Rome, Italy, June 1999.

4. Yamauchi, G. K., Burley, C. L., Mercker, E., Pengel, K., and Janakiram, R., "Flow Measurements of an Isolated Model Tilt Rotor," American Helicopter Society 55th Annual Forum, Montreal, Canada, May 1999.

5. Swanson, S. M.; McCluer, M. S.; Yamauchi, G. K.; and Swanson, A. A. "Airloads Measurements from a 1/4 - Scale Tiltrotor Wind Tunnel Test," 25th European Rotorcraft Forum, Rome, September 1999.

6. Booth, E. R., McCluer, M., and Tadghighi, H., *Acoustic Characteristics of an Isolated Tiltrotor Model in the DNW*, Journal of the American Helicopter Society Volume 46 Number 1, January 2001, pp. 72-80.

7. Burley, C. L., Brooks, T. F., Charles, B. D., and McCluer, M., "Tiltrotor Aeroacoustic Code (TRAC) Prediction Assessment and Initial Comparisons with TRAM Test Data," 25th European Rotorcraft Forum, Rome, Italy, September 1999.

8. Johnson, W. "Calculation of Tilt Rotor Aeroacoustic Model (TRAM DNW) Performance, Airloads, and Structural Loads," American Helicopter Society Aeromechanics Specialists' Meeting, Atlanta, Georgia, November 2000.

9. Zell, P. T. and Flack, K., "Performance and Test Section Flow Characteristics of the National Full-Scale Aerodynamics Complex 40- by 80-Foot Wind Tunnel," NASA TM 101065, February 1989.

10. Soderman, Paul T.; Schmitz, Fredric H.; Allen, Christopher S.; Jaeger, Stephen M.; Sacco, Joe N.; Hayes, Julie A., "Design of a Deep Acoustic Lining for the 40- by 80-foot Wind Tunnel Test Section," 20th AIAA/CEAS Aeroacoustics Conference, Bellevue, WA, May 1999.

11. Soderman, Paul T.; Jaeger, Stephen M.; Hayes, Julie A.; Allen, Christopher S., "Acoustic Performance of the 40- by 80- Foot Wind Tunnel Test Section Deep Acoustic Lining", 21st AIAA/CEAS Aeroacoustics Conference, Lahaina, HI, June 2000.

12. Warmbrodt, W., Smith, C. A., and Johnson, W., "Rotorcraft Research Testing in the National Full-Scale Aerodynamics Complex at NASA Ames Research Center," NASA-TM-86687, May 1985.

13. Johnson, W. J. "TRAM Physical Description," NASA Ames Research Center Report, (to be published).

14. Versteeg, M. H. J. B., and Slot, H., "Miniature Rotating Amplifier System for Wind Tunnel Application Packs 256 Pre-conditioning Channels in 187 Cubic Inch," Presented at the 17th International Congress on Instrumentation in Aerospace Simulation Facilities (ICIASF), Naval Postgraduate School, Monterey, California, September 29 - October 2, 1997.

15. Young, L. A., Lillie, D., McCluer, M., Derby, M., and Yamauchi, G., "Insights into Airframe Aerodynamics and Rotor-on-Wing Interactions from a Quarter-Scale Tiltrotor Wind Tunnel Model" American Helicopter Society Specialists' Conference, San Francisco, California, January 2001.

16. McVeigh, M. A., Grauer, P. E., and Paisley, D. J., "Rotor/Airframe Interactions on Tiltrotor Aircraft," American Helicopter Society 44th Annual Forum, Washington, D.C., June 1988.

17. Johnson, W. R., Helicopter Theory. Princeton University Press, New Jersey, 1980, pp. 290-293.

18. Wood, T. L., and Peryea, M. A., "Reduction of Tiltrotor Download," American Helicopter Society 49th Annual Forum, St. Louis, MO, May 1993.

19. Felker, F. F., and Light, J. W., "Rotor/Wing Aerodynamic Interactions in Hover," American Helicopter Society 42nd Annual Forum, 1986.

20. Keys, C. N., McVeigh, M. A., Dadone, L., and McHugh, F. J., "Considerations in the estimation of full-scale rotor performance from model rotor test data," American Helicopter Society 39th Annual Forum, St. Louis, MO, May 1983.

21. Burley, C. L., Marcolini, M. A., Brooks, T. F., Brand, A. C., and Conner, D. A., "Tiltrotor Aeroacoustic Code (TRAC) Predictions and Comparison with Measurements," American Helicopter Society 52nd Annual Forum, Washington, D.C., June 1996.

22. Johnson, W. "CAMRAD II, Comprehensive Analytical Model of Rotorcraft Aerodynamics and Dynamics." Johnson Aeronautics, Palo Alto, CA, 1999.

Appendix A. Solidity and Reynolds Number Corrections

This appendix describes how model data were scaled to full-scale V-22 performance levels by applying simple solidity (σ) and Reynolds number (Re) corrections to profile power (Cp_o). More information can be found in Keys[1], Johnson[2], Hoerner[3], and Schlichting[4].

Profile power is proportional to torque-weighted solidity and airfoil section drag coefficient.

$$Cp_o \propto \frac{\sigma \overline{c_d}}{8} \tag{1}$$

therefore:

$$\frac{Cp_{o2}}{Cp_{o1}} = \left(\frac{\sigma_2}{\sigma_1}\right)\left(\frac{\bar{c}_{d2}}{\bar{c}_{d1}}\right) \tag{2}$$

The mean drag coefficient ratio is a function of skin friction, and thus Reynolds number, Re. A simplified expression for skin friction with respect to Reynolds number for fully turbulent flow on an aerodynamically smooth surface (such as a well manufactured rotor blade) can be expressed as:

$$c_f = \frac{k}{(\mathrm{Re})^{1/M}} \tag{3}$$

where k is a constant and M ≈ 5 for Reynolds numbers between 10^6 and 10^7. Assuming that profile power is due largely to skin friction:

$$\left(\frac{\bar{c}_{d2}}{\bar{c}_{d1}}\right) \propto \left(\frac{c_{f2}}{c_{f1}}\right) \approx \left(\frac{\mathrm{Re}_1}{\mathrm{Re}_2}\right)^{1/5} \tag{4}$$

For simplicity, the Reynolds number is based on the rotor rotational speed at the 3/4 radius and blade geometry,

$$\mathrm{Re} = \frac{\rho V c}{\mu} \quad and \quad \sigma = \frac{bc}{\pi R} \tag{5}$$

where ρ = density, V = (0.75)Vtip, b is number of blades, c = effective blade chord, μ is kinematic viscosity, and R is rotor radius.

$$\mathrm{Re} = \frac{\rho .75 V_{tip}\left(\frac{\sigma \pi R}{b}\right)}{\mu} = \frac{\rho .75 V_{tip} \sigma \pi R}{\mu b} \tag{6}$$

Equation (2) can then be expressed as:

$$\frac{Cp_{o2}}{Cp_{o1}} = \left(\frac{\sigma_2}{\sigma_1}\right)\left\{\frac{\left(\frac{\rho(.75)V_{tip1}\sigma_1 \pi R_1}{\mu_1 b}\right)}{\left(\frac{\rho(.75)V_{tip2}\sigma_2 \pi R_2}{\mu_2 b}\right)}\right\}^{1/5} \tag{7}$$

Assume a reference of sea level and standard day conditions, ρ_0 = 0.0023769 slugs/ft^3, μ_0 = 3.7373 x 10^{-7} lb-sec/ft^2 and using Equation 7;

Rotor	R	σ	Vtip	Re ($x10^6$)	Cp_{o2}/Cp_{o1}
V-22	19.03	0.105	790	7.885	1.0
FS TRAM	4.75	0.105	705	1.756	0.7406
TRAM/DNW	4.75	0.105	705	1.756	0.7406
JVX/OARF	12.5	0.1138	760	5.400	0.8554
BHTI	2.85	0.105	789.5	1.180	0.6840
BVWT	2.85	0.1138	789.5	1.279	0.6413

Assuming that the induced power coefficient for all the rotors is approximately the same, a change in total power can be computed as follows:

$$Cp_{corrected} = Cp - Cp_o + Cp_{o\,corrected}$$

$$Cp_{corrected} = Cp - Cp_o\left(1 - \frac{Cp_{o\,corrected}}{Cp_o}\right) \tag{8}$$

$$\Delta Cp = -Cp_o\left(1 - \frac{Cp_{o2}}{Cp_{o1}}\right) \tag{9}$$

Rotor	Cp_o*	ΔCp
FS TRAM	0.00023	-0.00005967
TRAM/DNW	0.00018	-0.00004670
JVX/OARF	0.00018	-0.00002603
BHTI	0.00016	-0.00005057
BVWT	0.00024	-0.00008609

*where Cp_o is minimum model-scale profile power estimated from wind tunnel test data.

Figure of Merit (FM) can then be estimated using the corrected power coefficient.

$$FM_{corrected} = \frac{C_T^{3/2}}{\sqrt{2}\left(C_P + \Delta C_P\right)} \tag{10}$$

[1] Keys, C. N., et al, 39th AHS Forum, 1983, (Ref. 20)
[2] Johnson, W.R., "Helicopter Theory", Section 2-4.2.3
[3] Hoerner, "Fluid Dynamic Drag", 1965. Ch. 2, Sec. 4.
[4] Schlicting, "Grenzschichttheorie", 1951